858. Structural health monitoring (SHM) for composite structure undergoing tensile and thermal testing

F. Mustapha[1], K. D. Mohd Aris[2], N. A. Wardi[3], M. T. H. Sultan[4], A. Shahrjerdi[5]
[1, 3, 4]Department of Aerospace Engineering, Universiti Putra Malaysia, 43400 Serdang, Selangor, Malaysia
[2]Universiti Kuala Lumpur - Malaysian Institute of Aviation Technology
Jalan Jenderam Hulu, 43800 Dengkil, Selangor, Malaysia
[5]Department of Mechanical Engineering, Malayer University, Iran
E-mail: [1]*faizal@eng.upm.edu.my*, [2]*khdahri@miat.unikl.edu.my*, [3]*norainiwardi@gmail.com*, [4]*drthariq@gmail.com*, [5]*alishahrjerdi2000@yahoo.com*

(Received 20 June 2012; accepted 4 September 2012)

Abstract. Application of ultrasonic guided waves generated by piezoelectric smart transducers has become one of the widely-used techniques in structural health monitoring. This technique has led to significant improvements and profound effects in the field of aircraft reliability and safety. Lamb wave propagation on composite plate-like structure undergoing mechanical testing is investigated in the paper. Smart PZT actuator/sensor is bonded on the carbon-fiber and glass-fiber epoxy composites, which are subjected to tensile and thermal stress tests. The acquired results indicate the changes in scattering waves in composites materials due to the applied thermal and tensile force. Wavelet analysis was incorporated in this research work in order to distinguish different structural status.

Keywords: Lamb waves, structural health monitoring, piezoelectric transducer, composite structure, wavelet analysis.

Introduction

The safety in maintenance, repair and overhaul (MRO) for the aviation industry is paramount to ensure the compliance for the aircraft airworthiness at its highest level especially for civilian and air transport type aircrafts. A single unattended minor flaw or defect may lead to fatal catastrophic consequences and incur substantial financial losses [1]. There are many approaches in order to ensure the safety of air travel such as condition monitoring, scheduled inspections and reliability studies [2]. Nondestructive testing (NDT) is one of the most popular and very effective inspection techniques to monitor the damage and determine the level of defect. It can be noted that the inspection requires the aircraft to be grounded and demand the skills and manpower to perform the assessment. In other words, NDT is carried out only when a defect is detected or instructed [3].

Comprehensive and reliable monitoring methods are needed to detect the damage at the earlier stage. This is why researchers spent a significant effort to implement structural health monitoring (SHM) by using various techniques such as [4] Acoustic Emission (AE) through PZT transducers [5, 6], Fiber Bragg Grating (FBG) [7], Compact Vacuum Monitoring (CVM) [8] and Polyvinylidene fluoride (PVDF) [9] sensors. Currently motivations in investigating the SHM systems are studied from specimen to component levels. A recent novel method in SHM involves the integration of smart structures and materials [10, 11].

The primary motivation of SHM is to detect the anomaly of aircraft structure at the earliest stage as possible. Preventive steps can be taken at this stage and it will lead to cost saving and degree of repair needed. There are different procedures used to interpret the data retrieved from the SHM methods such as statistical analysis [12, 13], finite element [14, 15] and artificial intelligent protocols [16]. Among the methods stated, the statistical approach is much simpler to analyze, however it requires machine learning and a high amount of data analysis in order to ensure high data reliability [17]. A simple pattern comparison of a test signal with a baseline has shown an adequate promising result [18]. Moreover, the processed data is not convincing if

SHM wants to migrate to a real aircraft component application [19]. However, few steps need to be considered before SHM can mature.

At the present, most of the studies are focused on detecting structural damages. However, little research has been done on the characteristics of applied guided waves when subjected to tensile and thermal stresses. In this paper, the characteristics of applied Lamb waves generated and propagated in the composites structures were investigated in detail. The guided waves were introduced by a PZT sensor from the actuator to the receiver between two points placement. Any defects on the structures were identified by the change of the response signal. The signal also responded to the changes of structure composition whenever the specimen was yielding due to tensile force, or melting when additional heat is applied. Additional objective of this study was to investigate the differences of Lamb wave propagation in different materials. For that purpose, both tensile test and thermal stress have been carried out for CFEP and glass fiber composites.

Methodology

The methodology of the experiment is divided into several sections, which are the effect on tensile test with and without thermal loading on fiberglass reinforced plastic (FGEP) and carbon graphite reinforced plastic (CFEP).

Composite Specimen Fabrication

The specimens were made from plain weave fiberglass of Grade 200. The orientation was set as $[(0.90)]_{12}$. Epoxy-based resin was used to bind and cure the fiberglass together. Release agent or wax was applied to the mould surface to ensure an easy remolding. The laminates were fabricated one layer at a time by hand layup method on a rectangular mould made from aluminum block. Serrated edge roller and brush were used to even out the resin and discard any potential entrapped air. Pressure plate was used to aid the consolidation process during curing at room temperature for more than 24 hours. Once cured and remolded, the laminate was cut into 25 mm by 250 mm for mechanical testing purposes. The fabrication of the CFEP-epoxy resin also went through the same process.

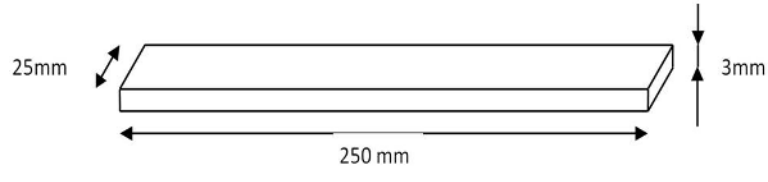

Fig. 1. Composite specimen (after cut)

Experimental Setup for Tensile Test

Tensile modulus and strength of the FGEP was measured in the longitudinal direction in accordance to ASTM D3039 [20]. The tensile specimens had a gage length of 250 mm and thickness of 3 mm. The test was performed using a MTS 100 kN machine at a constant rate of 2 mm/min. As the specimen experience the tension load, a deformation in specimen material will induce response. From the test, the strain data can be obtained and they are being determined from strain gauges attached directly to the specimen. Meanwhile, the integration of Testwork® software in the MTS Machine allowing the machine to record load distribution, displacements and time during the test. From all these data, dynamic stress-strain curve for specimen materials are determined and material behavior and properties under tensile load are described. Fig. 2 illustrates tensile test setup. The purpose of the strain gauge was to register the strain directly on

the specimen during the test. The operation of the strain gauge is based on the change of electrical resistance from the thin wire or piece of metal foil under strain. The sensor was bonded to the specimen in a specific direction. The wire and specimen shared the same strain thus, gave the reading momentarily when the load was applied.

Fig. 2. Test specimen with MTS Machine

Experimental Setup for Thermal-Stress Test

The thermal stress test was conducted by placing a pair of furnace at the designated location specimen. The instant thermal stresses were determined by the temperature distribution and generally much higher than those that occur in the steady state as shown in Fig. 3. During testing the heat transfer reduction effect is neglected due to close distance between the specimens and the heat source.

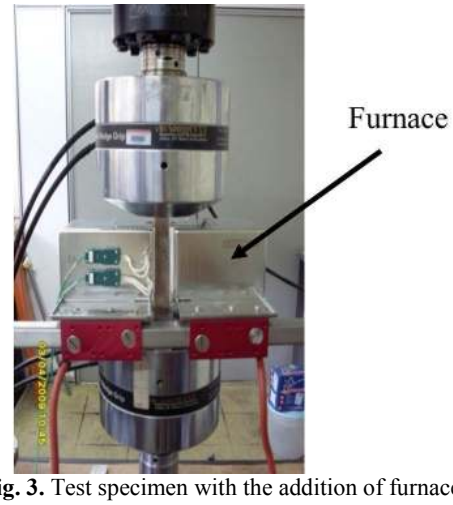

Fig. 3. Test specimen with the addition of furnace

PZT Sensors Placement

The PZT sensors were bonded by polyester/acrylic tape to the specimens which were connected to the Textronix machine wave generator at an output frequency of 250 kHz with 5 burst at 33 kHz. Fig. 4 shows the connection of the equipment.

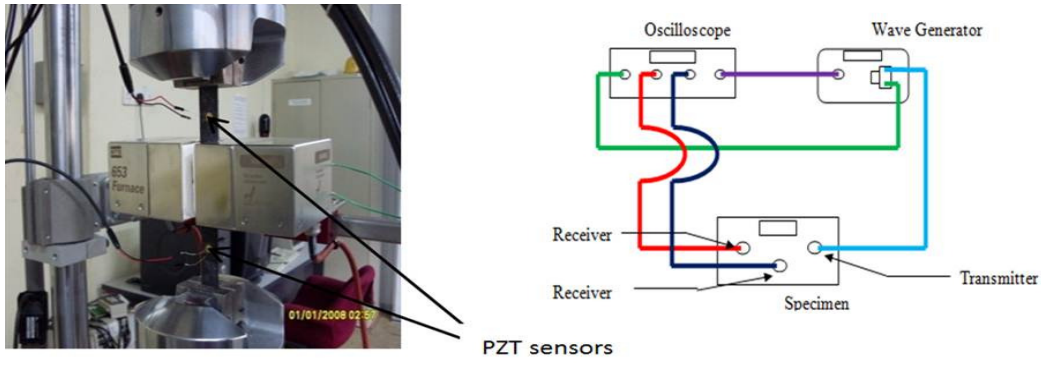

Fig. 4. Test specimen with the addition of PZT transducers

Wavelet Analysis

The waveforms from the PZT sensors are captured by the oscilloscope. The Lamb wave propagation is interpreted to analyze the V_{pp} of each condition. This is performed by acquiring the min and max values of V_{pp} and the wave pattern comparisons for feature extraction process. The continuous wavelet transform (CWT) analysis was executed to compare with the V_{pp} results. Morlet wavelet analysis was used to distinguish time based analysis with better visualization of the frequency-based distribution [19]. It is used to scrutinize the conditions particularly due to the nonstationary interrogating data investigated in the current work and the Gaussian pattern distribution [21].

Results and Discussion

The results are divided into several sections. Initially the oscilloscope captured about 5000 data points. The data points were then plotted by using SIGMAPLOT® software and a comparison of relevant graph was carried out by superimposed technique. By applying feature extraction process, only 2000 data points were plotted and superimposed because zone of interest lies within these areas. More detailed features were used by selecting the interest region with only 500 points for data extraction.

Tensile and Thermal Test Result

Stress-strain diagram for both FGEP and CFEP revealed the behavior of brittle materials under tensile load. A sudden drop at the end of the elastic curves depicted the total failure of the both FGEP and CFEP composite materials as shown in Fig. 5. The graph was segregated into three regions. Region 1 lies within the elastic region. Region 2 is just before reaching the ultimate stress and Region 3 is right after the breaking takes place. Fig. 5 indicates that there is a significant strength difference between the FGEP and CFEP. The strength of CFEP is twice as the FGEP panels.

However, the application of heat revealed a different behavior on the stress-strain diagram whereby there was no change in stress although the strain was increased such as shown in Fig. 6. Meanwhile, the effects of thermal condition prove a significant reduction in terms of strengths. The main reason is due to the use of low temperature (LT) epoxy resin. The typical LT resin cannot withstand high temperature due to the weak bonding of the resin molecules. The resin lost its integrity and breaks when the load is applied. Therefore the fibers solely carry the main stress until the structure fails.

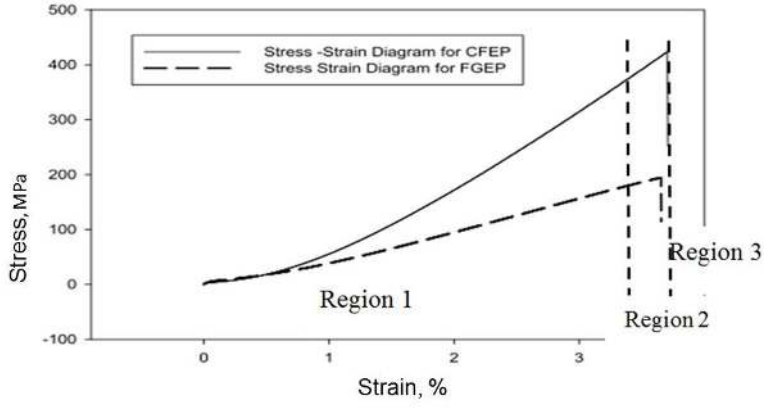

Fig. 5. Stress-strain diagram for FGEP and CFEP without thermal stress

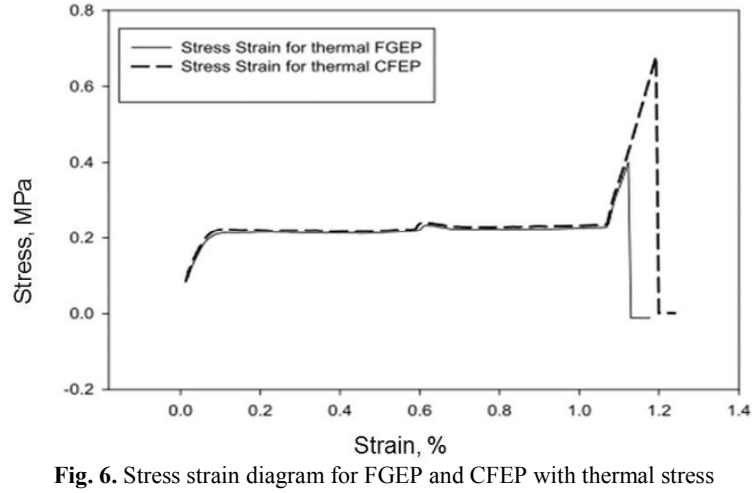

Fig. 6. Stress strain diagram for FGEP and CFEP with thermal stress

PZT Waveform Response for Tensile with and without Thermal Stress

Fig. 7 shows the input signal generated by the wave generator for all specimen conditions. The wave was monitored and calibrated each time before the specimens were tested.

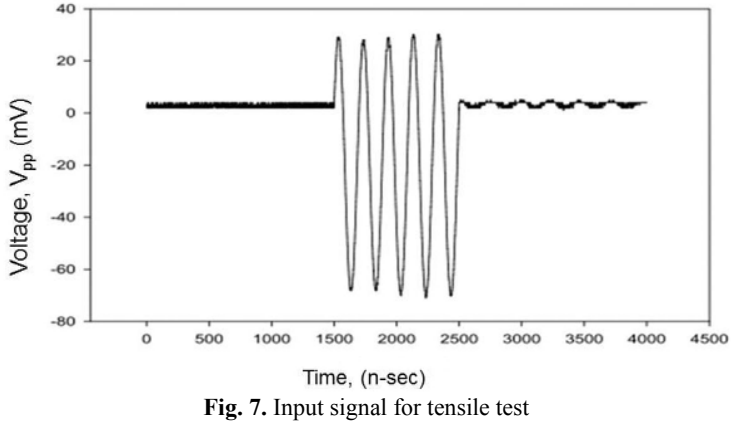

Fig. 7. Input signal for tensile test

FGEP without Thermal Stress

Figs. 8(a-c) present the condition at which the wave patterns were acquired and saved. The conditions which the data was taken were at the elastic range, momentarily before the total failure of the specimens and at the post failure. A typical mechanical failure was observed for all the specimens at the end of the test. At this stage the signal wave pattern lost its signals. Fig. 8c shows the signal lost and noise due to specimen rupture.

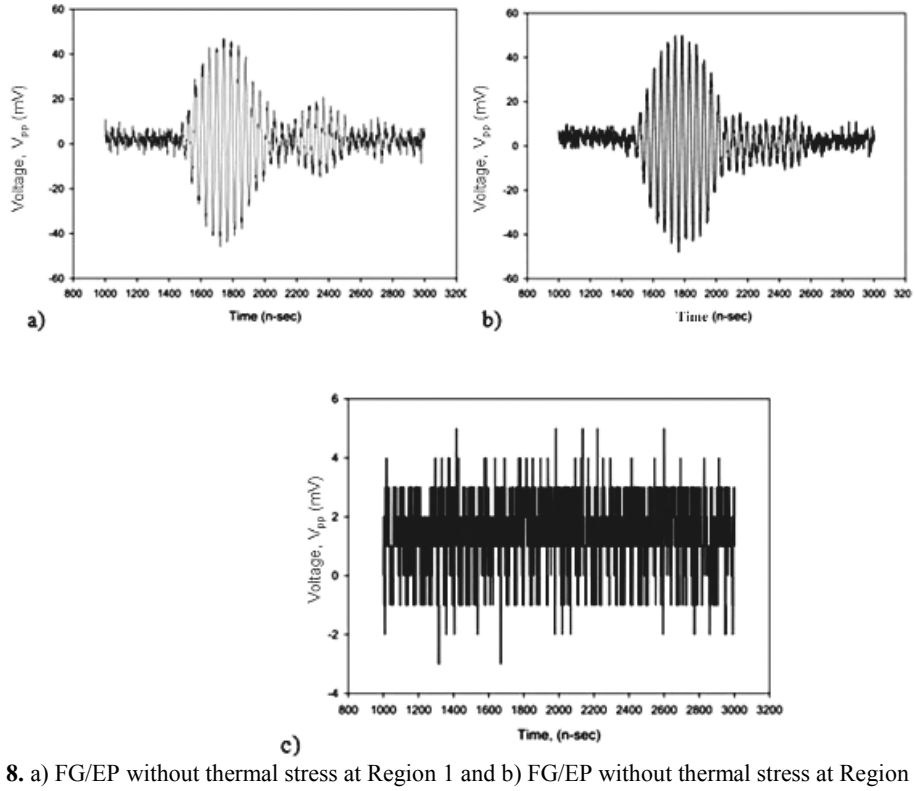

Fig. 8. a) FG/EP without thermal stress at Region 1 and b) FG/EP without thermal stress at Region 2 and c) FG/EP without thermal stress at Region 3

FGEP with Thermal Stress

The application of heat on specimen surfaces during tensile test has shown a different wave pattern. As been discussed in the stress strain diagram earlier, the significant difference in wave pattern was mainly due to the changing of the resin molecular structure. However, this change is also unique at the three observation points throughout the testing as shown in Figs. 9a-9c. Fig. 9c shows the behavior of the signal lost upon panel breakage.

CFEP with and without Thermal Stress

Observation of wave propagation on CFEP was carried out for both conditions (with and without thermal stress applied on the specimens during the tensile test). Similar behavior in terms of different wave patterns was observed at the three conditions. The results for CFEP without thermal stresses are shown in Figs. 10(a-c) and for CFEP with thermal stresses - in Figs. 11(a-c).

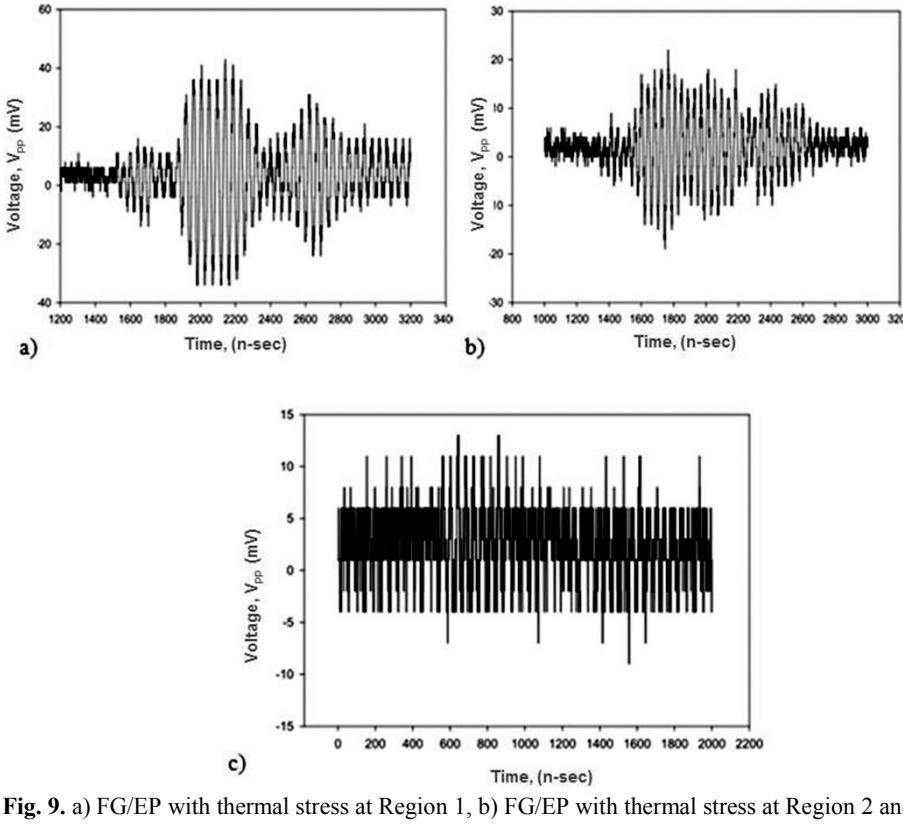

Fig. 9. a) FG/EP with thermal stress at Region 1, b) FG/EP with thermal stress at Region 2 and c) FG/EP with thermal stress at Region 3

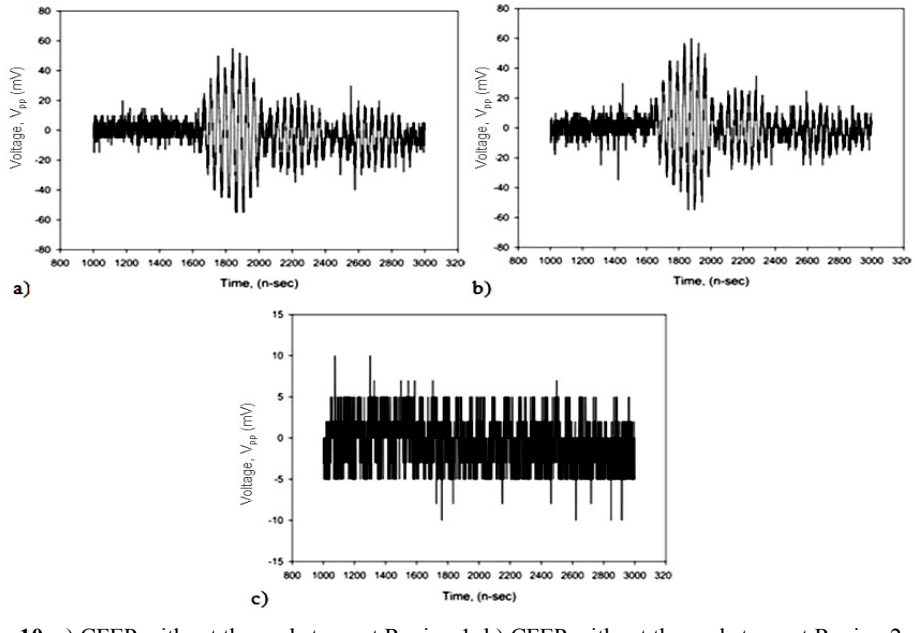

Fig. 10. a) CFEP without thermal stress at Region 1, b) CFEP without thermal stress at Region 2 and c) CFEP without thermal stress at Region 3

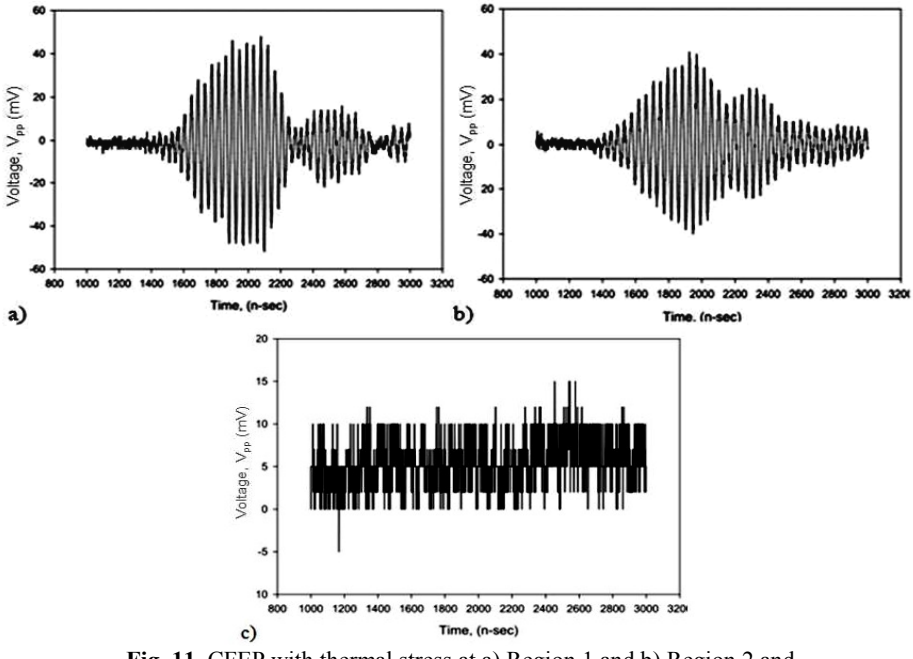

Fig. 11. CFEP with thermal stress at a) Region 1 and b) Region 2 and c) CFEP with thermal stress at Region 3

Feature Extraction

Further investigations were carried out in order to acquire more information on the signal transmission at the linear range of the stress-strain diagram and momentarily before the specimens break. Before the specimens break a low clicking sound was heard due to the fracture of individual fibers before the total rupture occurred. At this point the specimens loose their structural integrity and the behavior of the lamb wave revealed anomalies from the pristine condition. The conditions were compared for each individual specimen as shown in Figs. 12-15.

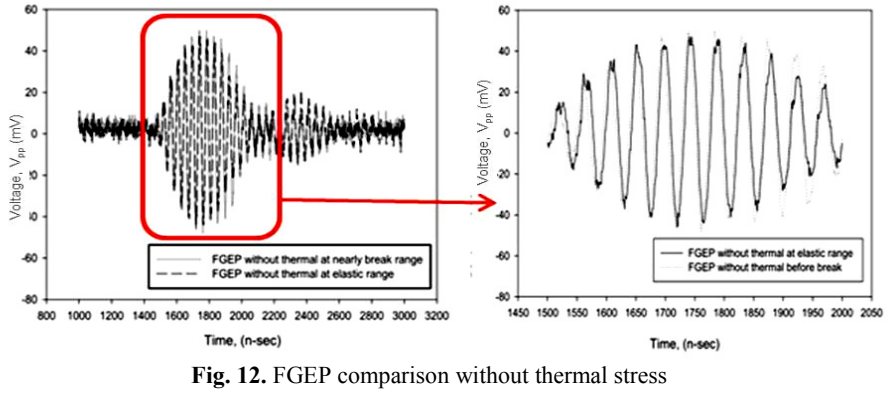

Fig. 12. FGEP comparison without thermal stress

Results of Wavelet Analysis

Wavelet analyses for both CFEP and FGEP with and without thermal influence are shown in Fig. 16. The signals are processed by using Autosignal employing Wavelet Filtering and

Construction function. The wavelet shows the frequency intensity of the receiving PZT sensors. Each of the wavelet intensity indicates a significant echo produced at the trailing of the signals. Since there is only a single attenuation during the interrogation process, the effect of thermal stresses produces significant trailing echo in which might have produced by the irregularities due to the heat applied. However at this stage, it is unknown to predict the strength and severity of the surface deterioration as it requires further investigation occurring at both Region 1 and II.

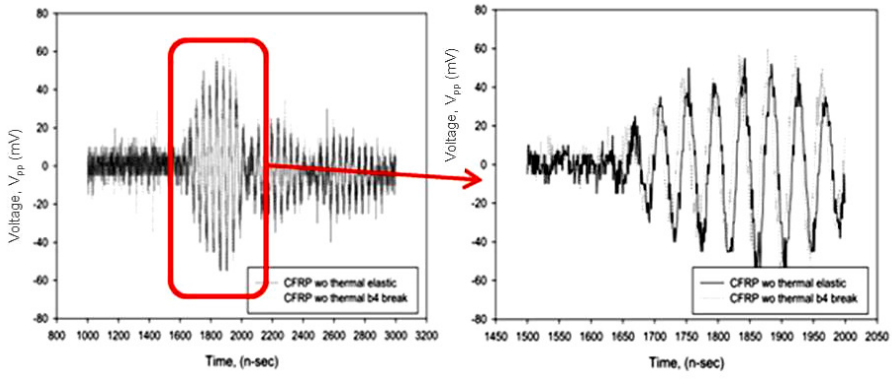

Fig. 13. FGEP comparison with thermal stress

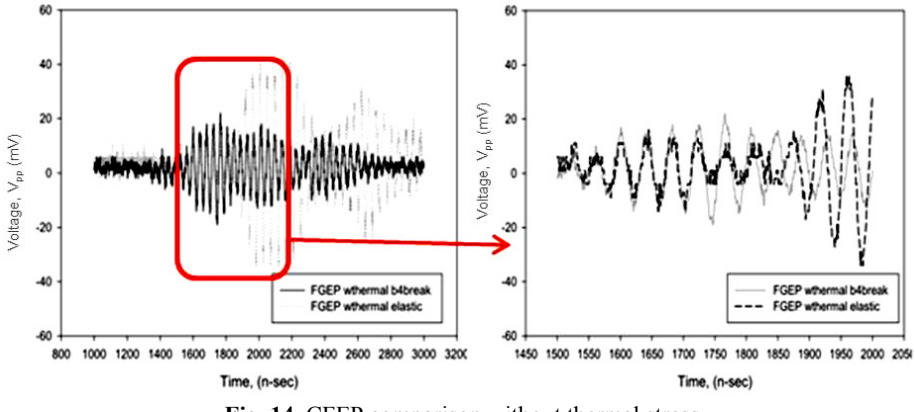

Fig. 14. CFEP comparison without thermal stress

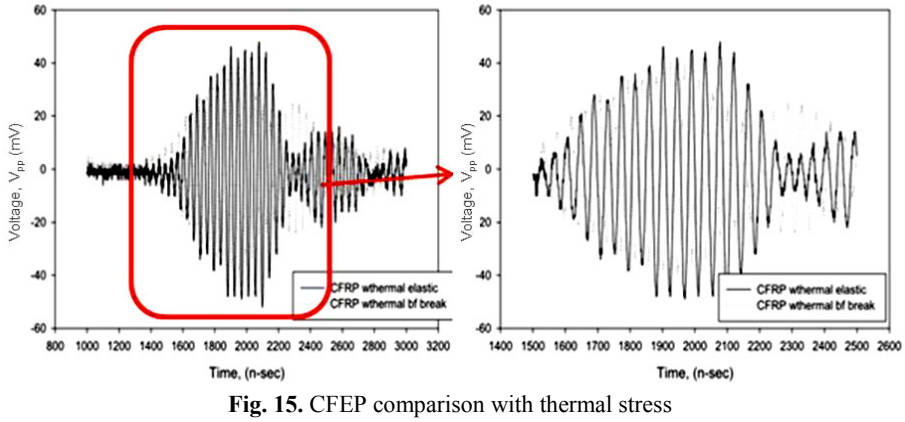

Fig. 15. CFEP comparison with thermal stress

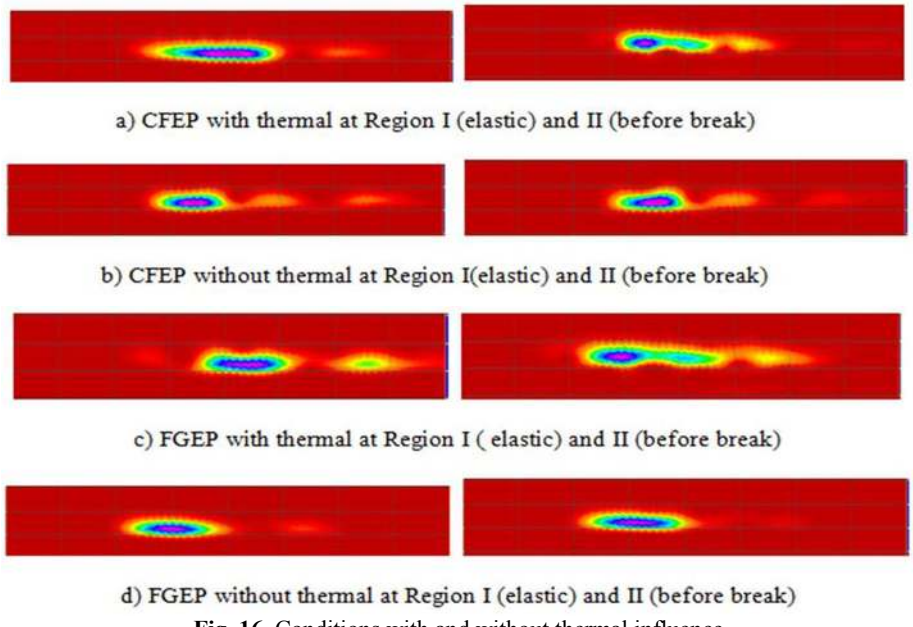

Fig. 16. Conditions with and without thermal influence

FT Analysis Using Damage Index (DI)

From the above feature extraction process, the signal spectrums were further filtered by using Matlab software through Fourier Transform (FT) analysis. The filtering process was applied to the conditions in order to find the mean value of the envelope response which is identified as the damage indexes perimeter. The damage indexes the highest value in which the frequency centroid corresponds to. From the results, the damage indexes (DI) were plotted to visualize prominent features of each condition. It was found that the DI at with the thermal applications shows a lower value for both CFEP and FGEP specimens. This was the indication of decreasing strength of the binder due to the heat influence. In addition, at Region 1 the values of the DI were higher compared to Region 2. This was due to the presence of the failure either at the matrix or the reinforcing fibers.

From the data obtained, a simple statistical analysis shows the distinctive pattern between the conditions with and without the thermal influence applied to the specimen. It is clear that the amplitude shape of wave response varies relatively with types of composites, and the presence loads varieties. For CFEP composite, the shape of wave packet is slightly different with and without the applied heat. When heat is applied to the specimen, the signals become inconsistent and unconditionally weaker. On the other hand, glass fiber composite experiencing different level of wave propagation through its structure as the signals become steadier and stronger when heat is applied during the test.

Due to fiber breakage after it reaches Region 3, the signal is no longer propagated through the structures when total failure occurs (as show in Fig. 8c, 9c, 10c and 11c). The noise propagation in those figures depicts as a noise at small scale. This is due to the fiber discontinuity that leads to discontinuity of the wave propagation on the surface. Moreover this is good indication because lost signals indicate a structural failure.

The thermal stress from the furnace played a significant factor on the wave signal behavior. The presence of heat change the microstructure of the specimens, particularly that of the resin. The resin becomes so hot that it disintegrates and breaks easily. The introduction of heat affects specimen microstructure, which leads to formations of weaker packet signals.

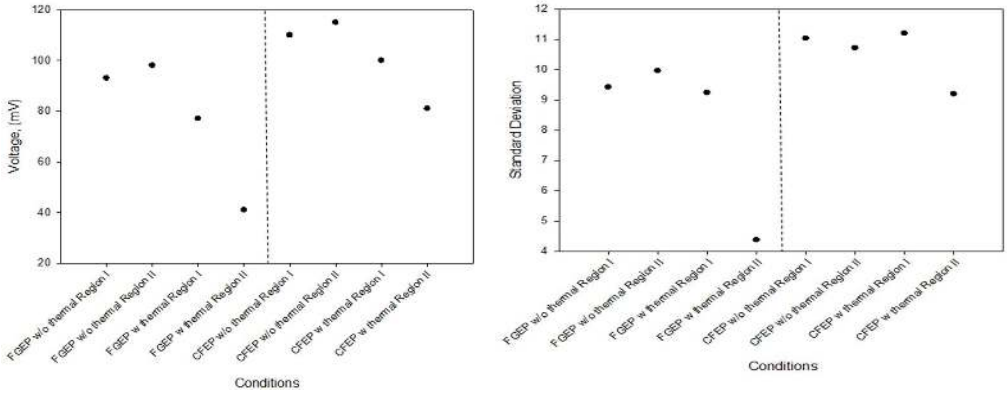

Fig. 17. FFT Analysis for Damage Index value

Thermal effect distinctly demonstrates the wavelet of the PZT sensors being distorted. This appeared due to the change of the grain/molecular structure altered by the heat. At Region 1, the wavelet reveals a similar pattern in which the low frequency and high frequency wavelet exist within the signal spectrum. However, when the materials nearly reach the breaking point (Region 2), both low frequency and high frequency wavelet coalesce. At this stage it is believed that micro-cracking of either resin or fiber breakage was initiated.

A slight change in V_{pp} is also observed. The changes in elongation and pre-break condition of the specimen structure caused amplitude of waveform become weaker. Compared to CFEP specimens, which were more dense, the wave propagation along the less dense glass fiber composites is not so well formed, even the signal packet can be clearly observed.

Conclusion

The ability of a specimen to spread wave signal depends on the arrangement of its microstructures. The higher the density of the specimen, the stronger is the wave propagation through it. When specific heat is applied in some specific times on specimen, the wave propagation is expected to be weaker or exhibit uncharacterized manner.

It was approved when CFEP composite was tested with and without application of heat. Even the strength of wave was not interrupted on the whole the presence of heat clearly changes the manner and characteristics of signal packet distribution. Glass fiber composite, on the other hand, did not exhibit the same principle. Instead of being weaker and having uncharacterized signal distribution, the wave signal that propagates throughout early-melt specimen are well-formed and better characterized. Therefore the stiffness of the material plays an important role in applicability of the SHM technique on a larger scale.

Finally, a simple comparison methodology may be adopted to observe and analyze significant effect on thermal stresses. Further investigation can confirm the consistency of these differences and further methodology through a comprehensive statistical pattern recognition method will be exploited by the authors of the paper in order to verify the result for a broader case study.

Therefore, it can be concluded that change of specimen microstructure affects the propagation of wave signal and yet, the type of specimen itself plays a major role as a factor contributing to characteristic wave propagation.

Acknowledgements

This work is supported by FRGS Grant number 5524003 from the Ministry of Higher Education (MOHE), Malaysia.

References

[1] **Charles R. Farrar, Keith Worden** An introduction to structural health monitoring. Phil. Trans. R. Soc. A, 2007, p. 303-315.

[2] **D. Chetwynd, F. Mustapha, K. Worden, J. A. Rongong, S. G. Pierce, J. M. Dulieu-Barton** Damage localization in a stiffened composite panel. Strain, Vol. 44, No. 4, 2008, p. 298-307.

[3] **J. D. Achenbach** Structural health monitoring – What is the prescription? Mechanics Research Communications, Vol. 36, No. 2, 2009, p. 137-142.

[4] **H. Sohn** A Review of Structural Health Monitoring Literature: 1996-2001. Los Alamos National Laboratory, 2004.

[5] **F. Mustapha, K. Worden, S. Pierce, G. Manson** Damage detection using stress waves and multivariate statistics: an experimental case study of an aircraft component. Strain, Vol. 43, No. 1, 2007, p. 47-53.

[6] **F. K. Chang, J. F. C. Markmiller, J. Yang, Y. Kim** Structural health monitoring. System Health Management, 2005, p. 419-428.

[7] **R. Jones, S. Galea** Health monitoring of composite repairs and joints using optical fibers. Composite Structures, Vol. 58, No. 3, 2002, p. 397-403.

[8] **A. Kousourakis, M. Bannister, A. Mouritz** Tensile and compressive properties of polymer laminates containing internal sensor cavities. Composites, Part A: Applied Science and Manufacturing, Vol. 39, No. 9, 2008, p. 1394-1403.

[9] **H. Bar, M. Bhat, C. Murthy** Identification of failure modes in GFGEP using PVDF sensors: ANN approach. Composite Structures, Vol. 65, No. 2, 2004, p. 231-237.

[10] **D. C. Betz, G. Thursby, B. Culshaw, W. J. Staszewki** Structural damage location with fiber Bragg grating rosettes and Lamb waves. Structural Health Monitoring, Vol. 6, No. 4, 2007, p. 299.

[11] **M. Yocum, H. Abramovich, A. Grunwald, S. Mall** Fully reversed electromechanical fatigue behavior of composite laminate with embedded piezoelectric actuator/sensor. Smart Materials and Structures, Vol. 12, 2003, p. 556.

[12] **K. Worden, G. Manson, N. Fieller** Damage detection using outlier analysis. Journal of Sound and Vibration, Vol. 229, No. 3, 2000, p. 647-667.

[13] **F. Mustapha, G. Manson, K. Worden, S. G. Pierce** Damage location in an isotropic plate using a vector of novelty indices. Mechanical Systems and Signal Processing, Vol. 21, No. 4, 2007, p. 1885-1906.

[14] **W. M. Ostachowicz** Damage detection of structures using spectral finite element method. Computers & Structures, Vol. 86, No. 3-5, 2008, p. 454-462.

[15] **A. Chattopadhyay, P. Peralta, A. Papandreou-Suppappola, Kovvali N.** A multidisciplinary approach to structural health monitoring and damage prognosis of aerospace hotspots. Aeronautical Journal, Vol. 113, No. 1150, 2009.

[16] **A. Kesavan, S. John, I. Herszberg** Structural health monitoring of composite structures using artificial intelligence protocols. Journal of Intelligent Material Systems and Structures, Vol. 19, No. 1, 2008, p. 63.

[17] **Mohd Aris K. D., Mustapha F., Sapuan S. M., Majid D. L.** A structural health monitoring of a pitch catch active sensing on PZT sensors on normal, damage and repair aircraft spoiler. Key Engineering Materials, Vols. 471-472, 2011, p. 1124-1129.

[18] **K. Diamanti, C. Soutis** Structural health monitoring techniques for aircraft composite structures. Progress in Aerospace Sciences, Vol. 46, No. 8, p. 342-352.

[19] **M. T. H. Sultan, W. J. Staszewski, K. Worden** Wavelet Feature Extraction for Impact Damage Analysis for CFEP Laminates.

[20] ASTM D3039/3039M, Annual Book of ASTM Standards. Vol. 08.01, ASTM, 2000.

[21] **Mohd Aris K. D., Mustapha F., Sapuan S. M., Majid D. L.** A Structural Health Monitoring of a Pitch Catch Active Sensing of PZT Sensors on CFRP Panels. A Preliminary Approach. Composite Materials / Book 2, Intech Publication, 2012.